DOI: 10.1111/echo.13651

REVIEW

WILEY Echocardiography

Echocardiographic assessment of the right ventricle in the current era: Application in clinical practice

Sridhar Venkatachalam MD, MRCP | Geru Wu MD, PhD | Masood Ahmad MD, FRCPC

Division of Cardiology, Department of Internal Medicine, University of Texas Medical Branch, Galveston, TX, USA

Correspondence
Masood Ahmad, Division of Cardiology, Department of Internal Medicine, University of Texas Medical Branch, Galveston, TX, USA.
Email: mahmad@utmb.edu

The right ventricle has unique structural and functional characteristics. It is now well recognized that the so-called forgotten ventricle is a key player in cardiovascular physiology. Furthermore, there is accumulating evidence that demonstrates right ventricular dysfunction as an important marker of morbidity and mortality in several commonly encountered clinical situations such as heart failure, pulmonary hypertension, pulmonary embolism, right ventricular myocardial infarction, and adult congenital heart disease. In contrast to the left ventricle, echocardiographic assessment of right ventricular function is more challenging as volume estimations are not possible without the use of three-dimensional (3D) echocardiography. Guidelines on chamber quantification provide a standardized approach to assessment of the right ventricle. The technique and limitations of each of the parameters for RV size and function need to be fully understood. In this era of multimodality imaging, echocardiography continues to remain a useful tool for the initial assessment and follow-up of patients with right heart pathology. Several novel approaches such as 3D and strain imaging of the right ventricle have expanded the usefulness of this indispensable modality.

KEYWORDS
3D echocardiography, clinical application, echocardiography, right ventricle

1 | INTRODUCTION

The right ventricle (RV) plays an important role in the pathophysiology of cardiopulmonary disease. Accurate assessment of RV structure and function is crucial to establishing prognosis and planning appropriate therapies. In this regard, two-dimensional (2D) echocardiography is often the first line and in some situations, the only noninvasive imaging modality for RV assessment, given its widespread availability and safety. However, the complex geometry of the RV presents a major challenge to echocardiographic interpretation. The most recent guidelines from the American Society of Echocardiography (ASE) provide a standardized approach to assessment of RV chamber size and function.[1] However, there are several limitations that need to be recognized to avoid potential misclassification. RV 2D strain and three-dimensional (3D) echocardiography are increasingly being used to complement routine 2D imaging. The objective of this review is to provide a practical approach to RV assessment in commonly encountered clinical situations based on the current evidence.

2 | RIGHT VENTRICULAR ANATOMY

The RV is the most anterior cardiac structure, located in close proximity to the sternum. In comparison with the left ventricle (LV), the RV is thin-walled, heavily trabeculated and has a complex 3D shape. Table 1 illustrates the important structural and functional differences between the right and left ventricles.[2] The RV consists of three distinguishable components: (1) the inlet comprises the tricuspid valve, chordae and papillary muscles, (2) the body with trabecular apex, and (3) the conus or the infundibulum. The conus and the pulmonic valve constitute the right ventricular outflow tract (RVOT). A high frequency transducer may help to optimize near-field imaging for the RV, and should be moved laterally to visualize the lateral free wall and apex. Similar to

 © 2017, Wiley Periodicals, Inc.

SHOUT
SHARE
IT

TABLE 1 Main structural and functional characteristics of the right and left ventricles[2]

Characteristic	Right ventricle	Left ventricle
Structure	Inflow region, trabeculated myocardium, infundibulum	No infundibulum, limited trabeculation
Shape	From the side: triangular; cross section: crescentic	Elliptic
End-diastolic volume (mL/m^2)	75±13	66±12
Ventricular wall thickness (mm)	2–5	7–11
Mass (g/m^2)	26±5	87±12
Ejection fraction (%)	>45%	>55%
Orientation of myofibers	Subepicardial: circumferentially; subendocardial: longitudinally	Subepicardial: obliquely; subendocardial: longitudinally; middle layers: circumferentially
Systolic pressure/diastolic pressure (mm Hg)	25/4	130/8
Pattern of contraction	Mainly longitudinal	Twisting and rotational
Stroke work index (g/m^2/beat)	8±2	50±20
Vascular resistance (dynes·sec·cm^{-5})	70 (20–130)	1100 (700–1600)
Adaptation to disease states	Better adaptation to volume overload states	Better adaptation to pressure overload states

Reproduced with permission from Elsevier.[2]

the LV, echocardiographic contrast agents may be used for improving endocardial definition of the RV.

3 | STANDARD ECHOCARDIOGRAPHIC VIEWS FOR THE RIGHT VENTRICLE

A comprehensive evaluation of the RV by 2D echocardiography obtains the six standardized views: parasternal long-axis (PLAX), parasternal RV inflow, parasternal short-axis (PSAX), apical four-chamber, RV-focused apical four-chamber, and subcostal views (Figure 1). Given the complexity of RV anatomy, each of the views provides additional information and should be used routinely. Table 2 provides a summary of the views and the key structures imaged. The RV walls are described as anterior, inferior, lateral, and the RV outflow tract (Figure 2).

4 | RIGHT VENTRICLE LINEAR AND AREA MEASUREMENTS

The RV-focused apical four-chamber view with the LV apex at the center of the scanning sector is the recommended view for measurements, reducing inter-observer variability (Figure 3).[3] The maximal basal (basal one-third of RV inflow), mid-cavity (middle third of RV inflow), and longitudinal RV dimensions are measured in this view (Table 3). Values >41 mm, >35 mm, and >83 mm are used to define RV enlargement, respectively (Table 4). Additionally, the RV end-diastolic and end-systolic areas may be obtained and indexed to body surface area (BSA). The normal values for RV areas indexed to BSA vary by gender (Table 4). RV area measurements are technically challenging and often result in underestimation or overestimation of RV size. The proximal and distal RV outflow tract (RVOT) diameters are measured using the PLAX and PSAX views (Table 3). Proximal RVOT diameter >30 mm by PLAX or >35 mm by PSAX and distal RVOT diameter >27 mm by PSAX represent RVOT enlargement (Table 4). As the reference values for linear dimensions are not indexed to body surface area (BSA), it is important to use them cautiously in those with larger BSA to avoid potential misclassification. Another simple albeit older method to estimate RV size is by comparison with left ventricular (LV) size. Calculation of RV to LV end-diastolic diameter ratio in the apical four-chamber view (abnormal if >1) or using both PLAX and apical four-chamber views (abnormal if >0.75) has been used in clinical studies.[4,5]

RV wall thickness is generally easy to obtain using the subcostal view (Table 3). The ASE guidelines specify that the site of measurement from the tricuspid annulus should be based on the approximate length of the anterior tricuspid valve leaflet when fully open.[3] To avoid overestimation, oblique sampling should be avoided. Furthermore, epicardial fat and trabeculae should be excluded.

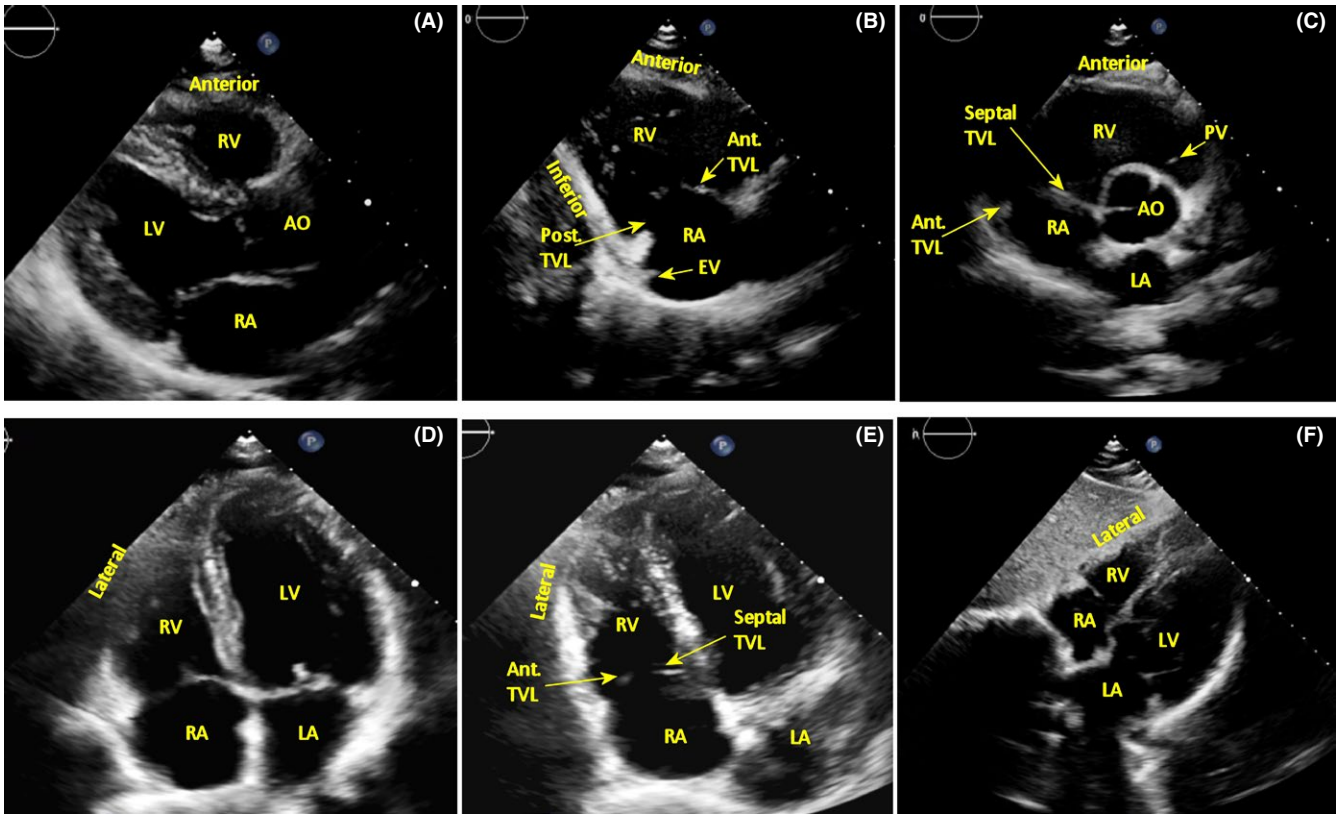

FIGURE 1 The six standardized views for the right ventricle: parasternal long-axis (A), parasternal RV inflow (B), parasternal short-axis (C), apical four-chamber (D), right ventricle-focused apical four-chamber (E), and subcostal views (F)

5 | ASSESSMENT OF RV SYSTOLIC FUNCTION USING 2D ECHOCARDIOGRAPHY

Given the impediments posed by the complex 3D structure of the RV, several nonvolumetric parameters that primarily evaluate longitudinal motion are commonly used to assess global or longitudinal RV function (Table 5). This is supported by the observation that the longitudinal vector of RV contraction is the most important given the orientation of the muscle fibers. The right ventricular index of myocardial performance (RIMP) and fractional area change (FAC) estimate global function (Table 5) and have established prognostic value in several clinical conditions as described subsequently. However, RIMP is not reliable in the setting of elevated RA pressure, and FAC neglects about 25%–30% of the RV volume in the outflow tract. RIMP values >0.43 by pulsed-wave Doppler or >0.54 by tissue Doppler imaging (TDI) suggest RV dysfunction. Using FAC, <35% area change indicates RV systolic dysfunction (Table 6). Tricuspid annular plane systolic excursion (TAPSE) by M-mode and peak systolic velocity (S-wave) of tricuspid annulus by pulsed-wave TDI have been validated against radionuclide ventriculography and may also provide prognostic information.[3] RV dysfunction is suggested by TAPSE values of <17 mm or S-wave velocity of <9.5 cm/s (Table 6). The main limitation is the partial representation of global RV function. The adaptation of LV 2D speckle tracking-derived global longitudinal strain (GLS) to assess for RV systolic function is relatively new, with reference values that are vendor-specific (Figure 4). To obtain RV GLS, the RV-focused apical view is chosen, and the peak value of three RV free wall segments is averaged. Alternatively, the average of three free wall and three septal segments could be used (Table 5). While TAPSE and pulsed-wave TDI are angle-dependent, speckle tracking is not. This is an important advantage especially in patients with dilated ventricles. However, the thin RV wall coupled with the not infrequent suboptimal image quality poses limitations to using RV GLS routinely.

6 | RV VOLUMETRIC MEASUREMENTS USING 3D ECHOCARDIOGRAPHY

The RV is unique from a functional standpoint with the inflow and outflow sections contracting perpendicularly to each other. While the RV inflow contracts longitudinally, the contraction in the RV outflow is circumferential. This function, combined with the complex morphology of the RV, limits adequate evaluation of global function using any of the 2D echocardiographic or Doppler-based methods described earlier. 3D echocardiography is well suited to evaluate RV end-diastolic volume, end-systolic volume, and therefore, RV ejection fraction (Figure 5, Movie S1). RV volumes need to be indexed to BSA, and the upper limits of normal are gender-specific. End-diastolic volumes >87 mL/m^2 for men and >74 mL/m^2 for women are indicative of RV enlargement (Table 4). Importantly, 3D echocardiography is validated against cardiac magnetic resonance imaging.[6,7] Identification of end-diastolic and end-systolic frames by 3D echocardiography must be based on maximal and minimal RV volumes, respectively, thus avoiding

TABLE 2 Important views in the assessment of the right heart[1]

Views	RV structures
PLAX of RV anterior wall	Anterior wall, proximal RVOT
PLAX of RV inflow	Anterior and inferior RV wall, anterior and posterior tricuspid valve leaflets, anterior and posterior papillary muscles, chordae, ostium of inferior vena cava, eustachian valve
PSAX of basal RV	Basal anterior RV wall, RVOT, tricuspid valve, pulmonic valve
Apical four-chamber	RV lateral wall and apex, RA
RV-focused apical four-chamber	RV lateral wall and apex, RA
RV subcostal four-chamber	RV lateral wall

PLAX=parasternal long-axis view; PSAX=parasternal short-axis view; RA=right atrium; RV=right ventricle; RVOT=right ventricular outflow tract.

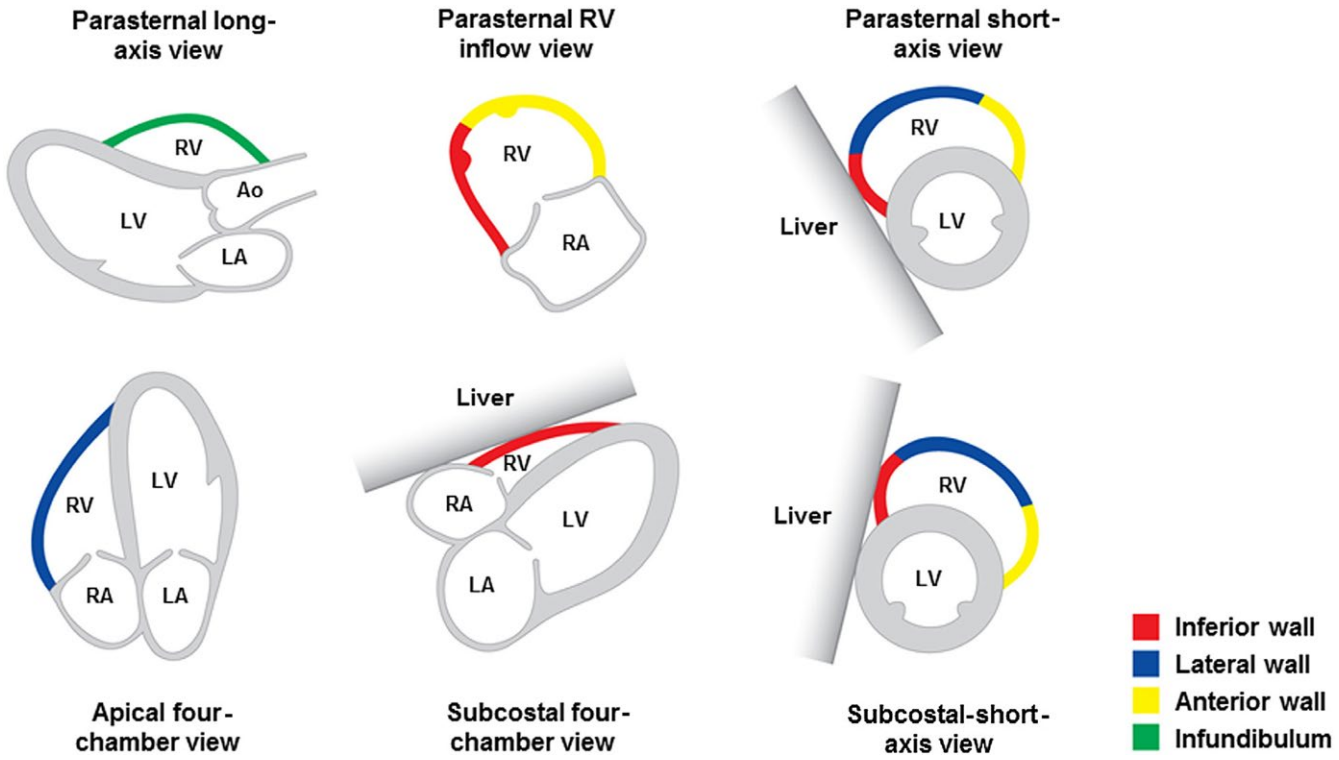

FIGURE 2 For echocardiographic analysis, the right ventricle (RV) is divided into four segments: the infundibulum, anterior wall, lateral wall, and inferior wall. The most useful projections for assessing RV function during stress echocardiography are presented. Ao, aorta; LA, left atrium; LV=left ventricle; RA=right atrium. Reproduced with permission from Elsevier[2]

the pitfall of using the LV for timing. Although volumetric assessment may not be necessary on a routine basis, 3D echocardiography is of benefit in post–cardiac surgery patients where 2D-based assessment of longitudinal function may not be reflective of global function.

7 | ECHOCARDIOGRAPHY FOR THE ASSESSMENT OF RV HEMODYNAMICS

Right ventricular function is dependent on preload, contractility, and afterload. The RV is thin-walled, operates under lower pressure conditions, and has a higher diastolic compliance compared to the LV. As wall stress is inversely correlated with wall thickness, the RV is more vulnerable to loading conditions especially acute increases in afterload. In this setting, the sudden increase in RV wall tension results in ventricular dilatation without a significant increase in RV end-diastolic pressure. However, with gradual increase in afterload, the RV exhibits considerable reserve and can even adapt to systemic pressure. Interventricular dependence is reflected by the flattening of interventricular septum during diastole with volume overload,[8] and predominantly during systole with severe pressure overload (Figure 6).[9] The distorted LV cavity takes the shape of *D* in the PSAX view at the mid-cavity level because of septal shift toward the center of the LV. Ryan et al. proposed the eccentricity index, defined as

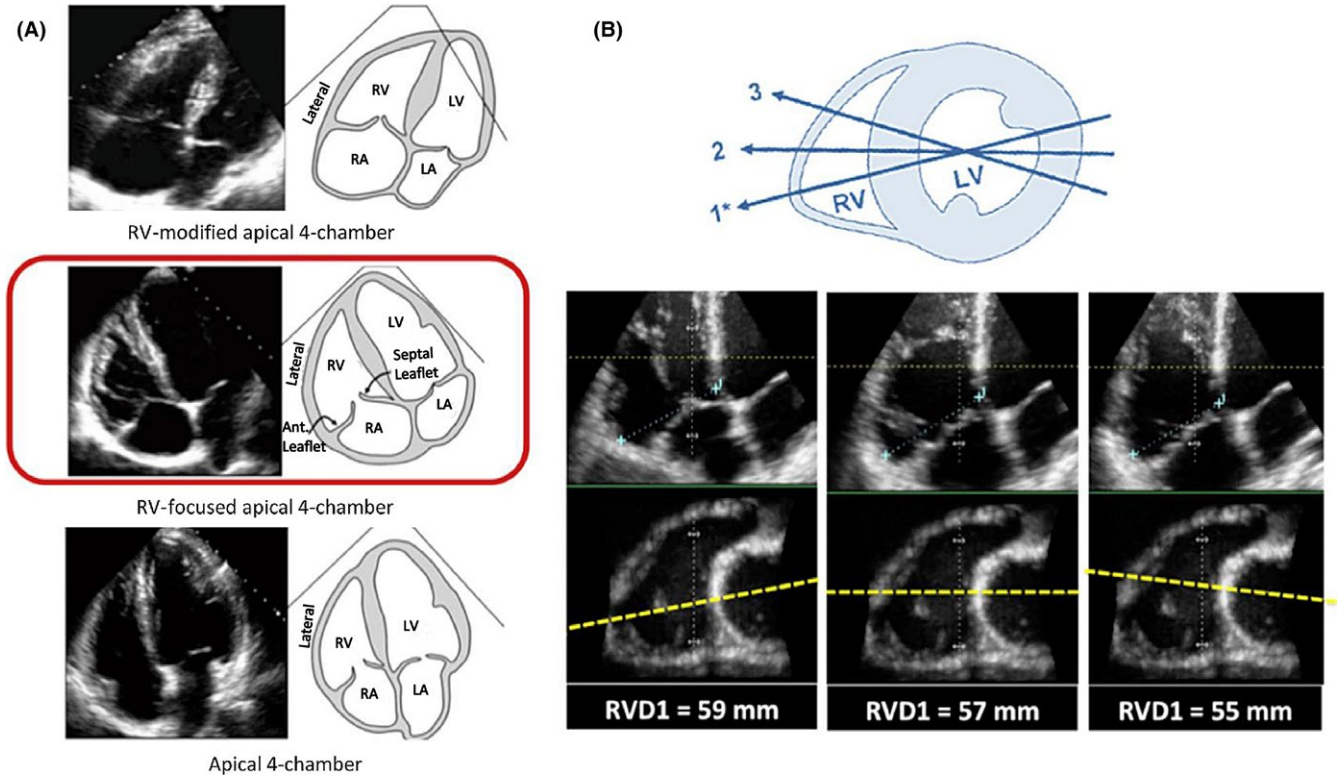

FIGURE 3 A. Three apical images demonstrating different views of the right ventricle (RV). The middle image shows the right ventricular-focused view. B. The rationale for maximizing the right ventricular basal dimension in the right ventricular-focused view. Below the cartoon, by manipulating offline the same 3D right ventricular data set, it is apparent that minor variations in the four-chamber plane position (dashed line) with respect to the right ventricular crescent shape may result in variability of right ventricular size when performed by linear measurements. Reproduced with permission from Elsevier[3]

TABLE 3 Echocardiographic assessment of RV size[3]

Parameter (Views)	Methods
RV inflow linear dimensions (RV-focused apical 4C view, at end-diastole)	Basal RV=maximum dimension in the basal one-third Mid-cavity RV=dimension in the middle third, at the level of papillary muscles
RV outflow linear dimensions (proximal: PLAX or PSAX; distal: PSAX. measured at end-diastole)	Proximal RVOT=dimension from the anterior RV wall to the interventricular septal-aortic junction (PLAX) or from the anterior RV wall to the aortic valve (PSAX) Distal RVOT=dimension just proximal to the pulmonary valve
RV wall thickness (subcostal view, at end-diastole using M-mode or 2DE)	Linear dimension of the RV free wall at a point that approximates the length of anterior tricuspid leaflet, excluding epicardial fat and trabeculae
RV inflow areas (RV-focused apical 4C view, at end-diastole and end-systole)	Area obtained by manual tracing of the entire RV endocardial border. Myocardial trabeculae, papillary muscles, and moderator band are included in the cavity
RV volumes by 3DE (apical 4C view, at end-diastole and end-systole)	Multibeat 3D acquisition with temporal resolution >20–25 volumes/sec. Myocardial trabeculae, papillary muscles, and moderator band are included in the cavity.

2DE=two-dimensional echocardiography; 3DE=three-dimensional echocardiography; 4C=four-chamber; RV=right ventricle.

TABLE 4 Normal values for RV chamber size[3]

Parameter	Mean±SD	Normal range
RV basal diameter (mm)	33±4	25–41
RV mid diameter (mm)	27±4	19–35
RV longitudinal diameter (mm)	71±6	59–83
RVOT PLAX diameter (mm)	25±2.5	20–30
RVOT proximal diameter (mm)	28±3.5	21–35
RVOT distal diameter (mm)	22±2.5	17–27
RV wall thickness (mm)	3±1	1–5
RVOT EDA (cm^2)		
Men	17±3.5	10–24
Women	14±3	8–20
RV EDA indexed to BSA (cm^2/m^2)		
Men	8.8±1.9	5–12.6
Women	8.0±1.75	4.5–11.5
RV ESA (cm^2)		
Men	9±3	3–15
Women	7±2	3–11
RV ESA indexed to BSA (cm^2/m^2)		
Men	4.7±1.35	2.0–7.4
Women	4.0±1.2	1.6–6.4
RV EDV indexed to BSA (mL/m^2)		
Men	61±13	35–87
Women	53±10.5	32–74
RV ESV indexed to BSA (mL/m^2)		
Men	27±8.5	10–44
Women	22±7	8–36

EDA=end-diastolic area; ESA=end-systolic area; PLAX=parasternal long-axis view; RVOT=RV outflow tract.
Reproduced with permission from Elsevier.[3]

the ratio of two perpendicular minor-axis diameters of the LV cavity measured in systole and diastole.[10] A value >1.0 is considered abnormal and may be useful to distinguish RV volume overload from pressure overload.[10]

8 | ECHOCARDIOGRAPHIC ASSESSMENT OF THE RV IN CLINICAL PRACTICE

A routine echocardiographic examination should always include the six views described above to characterize the RV. A comprehensive assessment of RV systolic function is time-consuming and generally not required in all patients. However, clinicians often encounter situations where assessment of RV function in warranted based on the initial echocardiographic findings or the clinical status of the patient. The following is a review of RV assessment in commonly encountered clinical conditions, using echocardiographic data published in literature.

8.1 | Advanced heart failure

Patients in refractory heart failure with reduced ejection fraction (Stage D), represent an important subset of patients who may benefit from advanced management strategies such as implantation of a left ventricular assist device (LVAD) as a bridge to transplantation or as destination therapy. Evidence of RV failure is an important risk factor for mortality in LVAD recipients based on the Interagency Registry for Mechanically Assisted Circulatory Support (INTERMACS) data.[11,12] Therefore, RV failure especially if severe is a contraindication for LVAD[13] or may be considered for biventricular assist device (BiVAD). Estimation of RV volume and ejection fraction using 3D echocardiography is recommended by the ASE if available, for accurate assessment prior to LVAD implantation (Movie S2).[14,15] It is important to note that decision making with regard to biventricular assist device vs LVAD, should not rely solely on echocardiographic signs. As described in the

TABLE 5 Echocardiographic assessment of RV function[3]

Parameter (Views)	Methods
RV global function—RIMP (apical 4C and PSAX views)	By pulsed Doppler: RIMP=(TCO−ET)/ET By tissue Doppler: RIMP=(IVRT+IVCT)/ET=(TCO−ET)/ET
RV global systolic function—FAC (RV-focused apical 4C view, at end-diastole and end-systole)	RV-FAC (%)=100×(EDA−ESA)/EDA
RV longitudinal systolic function—TAPSE (M-mode)	Tricuspid annular longitudinal excursion measured between peak systole and end-diastole
RV longitudinal systolic function—pulsed tissue Doppler S-wave (apical 4C)	Peak systolic velocity of tricuspid annulus
RV longitudinal systolic function—GLS (RV-focused apical 4C view)	Peak systolic 2D strain imaging, averaged over three segments (RV free wall) or six segments (three free wall and three septal)
RV ejection fraction by 3DE	RV EF (%)=100×(EDV−ESV)/EDV

2D=two-dimensional; 3DE=three-dimensional echocardiography; 4C=four-chamber; EDA=end-diastolic area; ESA=end-systolic area; ET=ejection time; FAC=fractional area change; GLS=global longitudinal strain; IVCT=isovolumic contraction time; IVRT=isovolumic relaxation time; PSAX=parasternal short-axis; RIMP=right ventricular index of myocardial performance; RV=right ventricle; TAPSE=tricuspid annular plane systolic excursion; TCO=tricuspid valve closure-to-opening time.

TABLE 6 Normal values for parameters of RV function[3]

Parameter	Mean±SD	Abnormality threshold
TAPSE (mm)	24±3.5	<17
Pulsed Doppler S-wave (cm/s)	14.1±2.3	<9.5
Color Doppler S-wave (cm/s)	9.7±1.85	<6.0
RV fractional area change (%)	49±7	<35
RV free wall 2D strain (%)[a]	−29±4.5	>−20[b]
RV 3D EF (%)	58±6.5	<45
Pulsed Doppler MPI	0.26±0.085	>0.43
Tissue Doppler MPI	0.38±0.08	>0.54
E-wave deceleration time (ms)	180±31	<119 or >242
E/A	1.4±0.3	<0.8 or >2.0
e′/a′	1.18±0.33	<0.52
e′	14.0±3.1	<7.8
E/e′	4.0±1.0	>6.0

MPI=Myocardial performance index.
[a]Limited data; values may vary depending on vendor and software version.
[b]<20 in magnitude with the negative sign.
Reproduced with permission from Elsevier.[3]

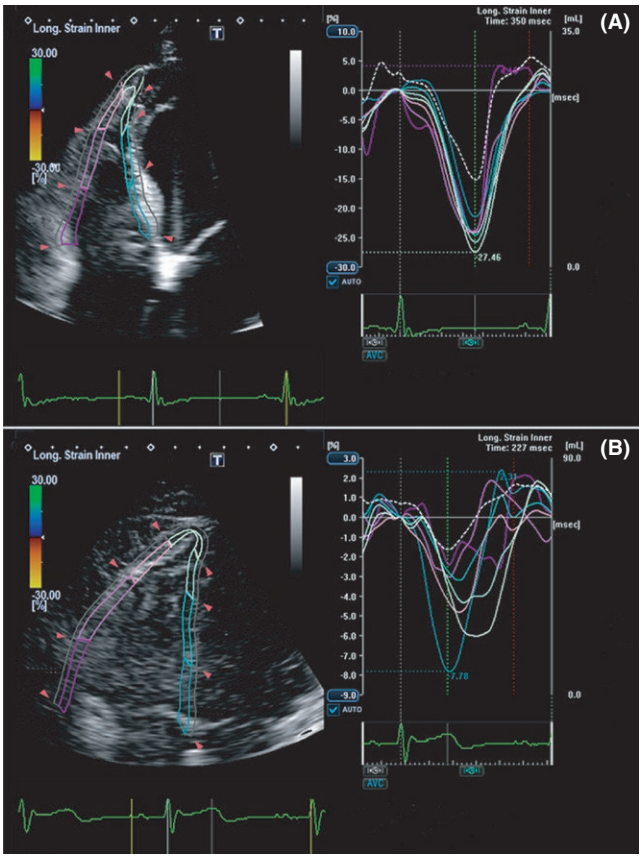

FIGURE 4 Speckle tracking two-dimensional (2D) longitudinal strain imaging in a normal subject (A) and patient with right ventricular (RV) dysfunction (B). Toshiba 2D Wall Motion Tracking software (Toshiba Medical Systems) was adapted for RV strain analysis. Using the apical four-chamber RV-focused view, the RV borders were manually traced. Speckle tracking was semi-automated. Global longitudinal strain analyses were performed using seven segments to represent RV: three free wall segments, three septal segments, and one apical segment. The peak systolic strain values of the seven segments were averaged to derive global RV longitudinal strain, −15% in Panel A (normal), and −5% in Panel B (RV dysfunction)

ASE recommendations, qualitative assessment of RV size and function may be sufficient in patients that have clinical symptoms and signs for right-sided heart failure.[14] Long-term survival is significantly improved when patients with clinical and echocardiographic signs for right ventricular systolic dysfunction proceed to planned biventricular assist device implantation.[16]

Despite preoperative assessment, RV failure may be detected post LVAD implantation in 9%–44% of patients.[17] Among the nonvolumetric echocardiographic surrogates for RV function, RV free wall peak longitudinal strain (absolute value <9.6%), tricuspid valve annular dilation (≥23 mm/m^2), and RV:LV end-diastolic diameter ratio (≥0.75) have been shown to be independent predictors of RV failure after LVAD implantation.[5,18,19] In a multivariable model, TAPSE did not have significant predictive value,[18] as severe LV dysfunction may contribute to rocking motion resulting in falsely normal value. Although RV-pulse-wave TDI (S′<4.4 cm/s and RV E/E′>10) was shown to be predictive in one univariate analysis,[20] the main limitation is angle dependency. The use of more than one predictor to assess for RV function is preferable in the absence of volumetric estimation.[14,20] Table 7 summarizes the echocardiographic variables predictive for RV failure in the LVAD patient population.[21]

Perioperative transesophageal echocardiography (TEE) during LVAD implantation is imperative as air may get entrapped during the LV coring procedure, or air may appear in left-sided chambers during re-initiation of mechanical ventilation after cardiopulmonary bypass. Air embolization to the right coronary artery (RCA) often results in acute RV dysfunction or dilatation. Acute severe tricuspid regurgitation (TR) may be noted as a secondary complication. If RV dysfunction does not improve after a period of watchful waiting, de-airing maneuvers need to be instituted.[14,22] In the postoperative period, right heart failure is an important and frequent cause of morbidity and mortality.[17] Movie S3 demonstrates severe RV dysfunction in the immediate postoperative period after LVAD implantation, with subsequent improvement (Movie S4). There are no universal diagnostic criteria for right heart failure in the LVAD population. Available criteria have used a combination of clinical, hemodynamic, or inotropic parameters (Table 7).[17,23] Assessment of RV size, function, or severity of TR by echocardiography is necessary to complement hemodynamic data.

8.2 | Pulmonary hypertension

A mean pulmonary artery (PA) pressure >25 mm Hg by invasive measurement is used to define pulmonary hypertension (PH). However, in

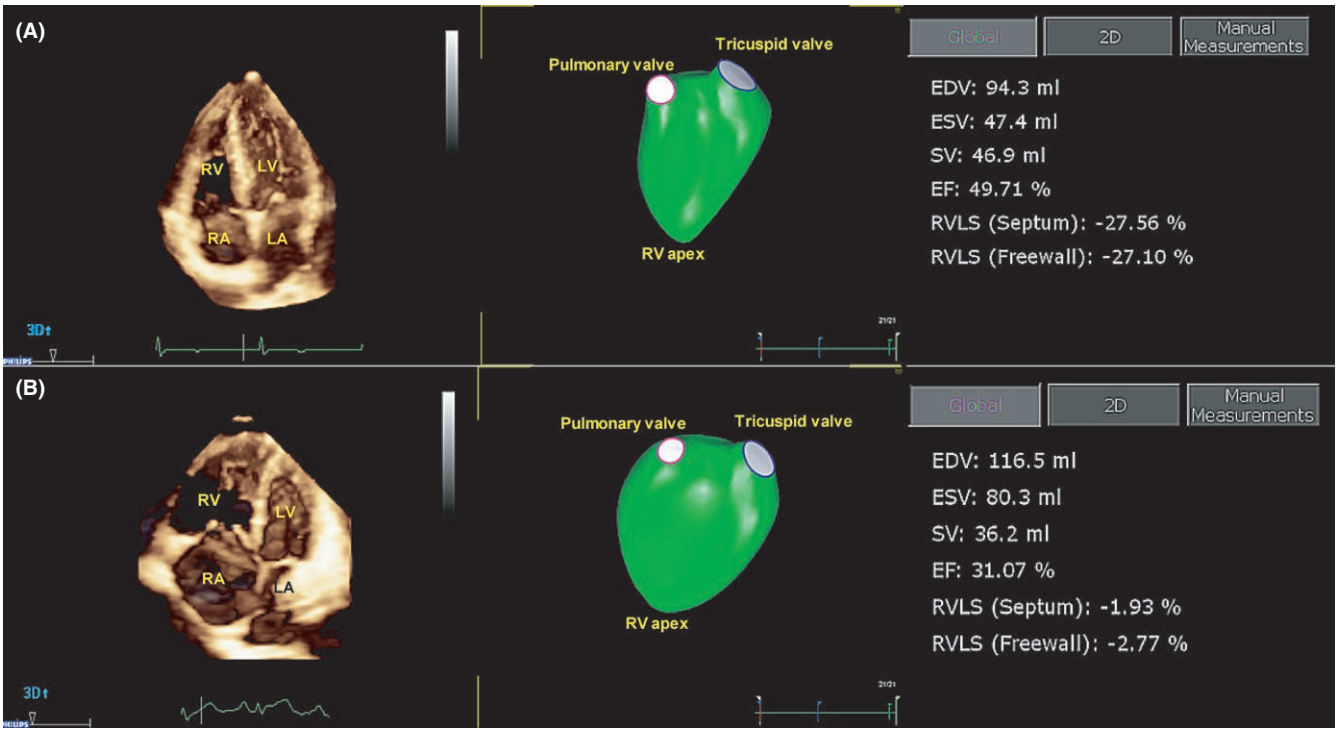

FIGURE 5 3D full-volume acquisition to calculate right ventricular (RV) end-diastolic volume (EDV), RV end-systolic volume (ESV) and RV ejection fraction (EF). A. Represents the four-chamber view in end-diastole and the end-diastolic 3D RV model generated using a semi-automatic border detection algorithm in a normal subject with RV EF=49.7%. B. Represents RV dysfunction with RV EF=31%

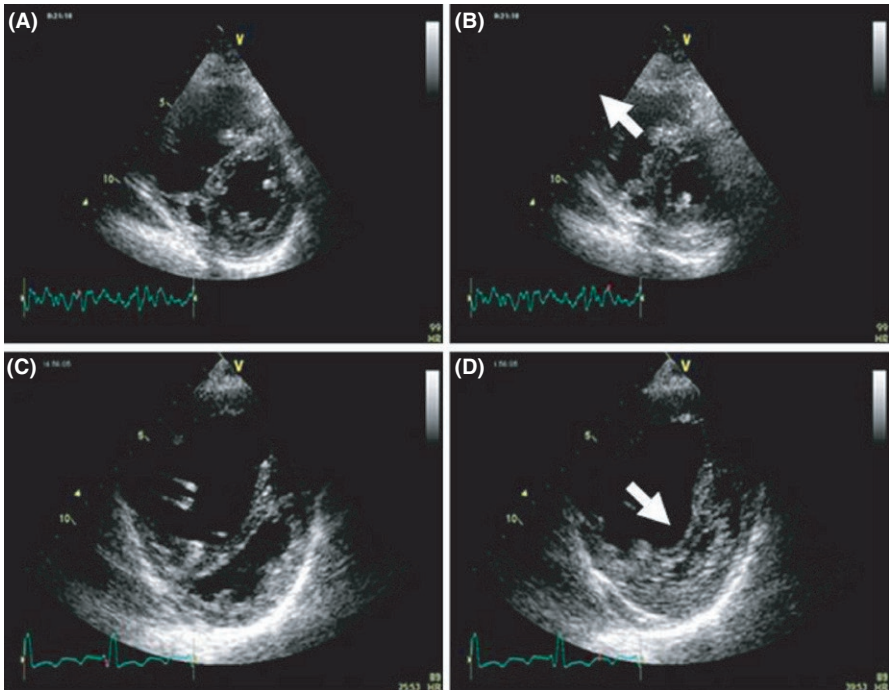

FIGURE 6 Parasternal short-axis views at the mid-ventricular level. A, B. Patient with atrial septal defect type ostium secundum, consequent right ventricular volume overload, and mildly elevated pulmonary artery pressures—flattening of the interventricular septum at end-diastole (A) and recovering of shape at end-systole (arrow) (B). C, D. Patient with severe pulmonary arterial hypertension and consequent severe right ventricular pressure overload—flattening of the interventricular septum both at end-diastole (C) and end-systole (arrow) (D). Reproduced with permission from Oxford University Press[9]

the initial assessment of patients with suspected PH, echocardiography is the most appropriate first-line diagnostic test. The mean PA pressure can be derived by echocardiography using the estimated PA systolic pressure (PASP) and PA diastolic pressure (PADP) or alternatively from the PA acceleration time (abnormal if <100 ms). More commonly, however, the right ventricular systolic pressure (RVSP) is reported and used to assess for PH because RVSP equals PASP in the absence of RVOT obstruction or pulmonic valve stenosis. An optimal TR jet that has the best envelope and maximal velocity is crucial to reliably determine RVSP using the equation: 4×(peak TR jet velocity)^2+right atrial pressure. Multiple and sometimes off-axis views are necessary to achieve an accurate measurement.[24] As peak TR jet

TABLE 7 Echocardiographic variables predicting right ventricular failure after left ventricular assist device placement[21]

Study (first author)	Patients (No.)	VAD type	BTT (%)	RVF definition	RVF incidence (%)	Risk factors
Puwanant[72]	33	Pulsatile 55% Continuous 45%	67	≥14 d inotropes or pulmonary vasodilators	33	Tricuspid annular motion <7.5 mm
Potapov[73]	54	Pulsatile 43% Continuous 57%	-	Need for RVAD or 2 of: MAP <55 mm Hg, CVP >16 mm Hg, mixed venous sat <55%, cardiac index <2 L/min/m^2, inotropic support >20 units	17	RV short-/long-axis ratio >0.6 (OR 4.4) Grade III/IV tricuspid regurgitation (OR 4.7)
Kukucka[74]	115	Continuous	-	Need for RVAD or 2 of MAP <55 mm Hg, CVP >16 mm Hg, mixed venous saturation <55%, cardiac index <2 liters/min/m^2, inotropic support >20 units	13	TEE measured RV/LV end-diastolic diameter ratio >0.72 (OR 11.4)
Vivo[5]	109	Continuous	49	Need for RVAD, ≥14 d inotropes	23	TTE measured RV/LV end-diastolic diameter ratio >0.75 (OR 5.4)
Kato[75]	111	Pulsatile Continuous	-	Need for RVAD, ≥14 d inotropes, inhaled nitric oxide ≥48 h	32	LVEDD >74 mm (OR 0.6) LVEF >22% (OR 2.3) LAD/LVEDD ratio >0.66 (OR 2.0)
Grant[18]	117	Continuous	67	Need for RVAD, ≥14 d inotropes	40	RV peak longitudinal strain >−9.6%
Cameli[76]	10	Continuous	-	Need for RVAD, ≥14 d inotropes, inhaled nitric oxide ≥48 h, late inotropic support starting >14 d after implant	30	Depressed free wall RV longitudinal strain

BTT=bridge to transplant; CVP=central venous pressure; LAD=left atrial diameter; LVEDD=left ventricular end-diastolic diameter; LVEF=left ventricular ejection fraction; MAP=mean arterial pressure; RV=right ventricle; RVAD=right ventricular assist device; RVF=right ventricular failure; TEE=transesophageal echocardiography; TTE=transthoracic echocardiography; VAD=ventricular assist device.
Reproduced with permission from Elsevier.[21]

TABLE 8 A. Echocardiographic probability of pulmonary hypertension in symptomatic patients with a suspicion of pulmonary hypertension.[30] B. Echocardiographic signs suggesting pulmonary hypertension used to assess the probability of pulmonary hypertension in addition to tricuspid regurgitation velocity measurement in Table A[30]

(A)		
Peak tricuspid regurgitation velocity (m/s)	**Presence of other echo pulmonary hypertension signs[a]**	**Echocardiographic probability of pulmonary hypertension**
≤2.8 or not measurable	No	Low
≤2.8 or not measurable	Yes	Intermediate
2.9–3.4	No	
2.9–3.4	Yes	High
>3.4	Not required	

(B)		
a: The ventricles[b]	**b: Pulmonary artery[b]**	**c: Inferior vena cava/right atrium[b]**
Right ventricle/left ventricle basal diameter ratio >1.0	Right ventricular outflow Doppler acceleration time <105 msec and/or mid-systolic notching	Inferior vena cava diameter >21 mm with decreased inspiratory collapse (<50% with a sniff or <20% with quiet inspiration)
Flattening of the interventricular septum (left ventricular eccentricity index >1.1 in systole and/or diastole	Early diastolic pulmonary regurgitation velocity >2.2 m/sec	Right atrial area (end-systole) >18 cm^2
	PA diameter >25 mm	

[a]See Table B. Reproduced with permission from Oxford University Press[30]

[b]Echocardiographic signs from at least two different categories (a/b/c) from the list should be present to alter the level of echocardiographic probability of pulmonary hypertension. Reproduced with permission from Oxford University Press.[30]

velocity is squared when calculating RVSP, it is important that only the dense portion of the spectral Doppler signal be used to avoid any overestimation. A common pitfall when using agitated saline contrast to enhance TR jet is overestimation, resulting from noise that obscures the underlying clear envelope. Conversely, very severe TR may lead to underestimation of RVSP because of early equalization of pressures leading to Doppler envelope cutoff.[1] The ASE guidelines state normal resting values of ≤2.8–2.9 m/s for the peak TR gradient.[1] This corresponds to an RVSP of 35–36 mm Hg assuming RA pressures between 3 and 5 mm Hg. In the assessment of unexplained dyspnea, RVSP >40 mm Hg by echocardiography warrants further evaluation.[25] Because the upper limit of normal among older (age >50 years) or obese (body mass index >30 kg/m^2) individuals may include 40 mm Hg, using age and body mass index corrected values is preferable.[24,26] Pulmonary vascular resistance (PVR) may also be derived by echocardiography using TR jet velocity and RVOT time-velocity integral (TVI). Although few studies have shown good correlation with invasive measurements,[27,28] PVR by echocardiography should not replace right heart catheterization for therapeutic decision making.[1] Pulsed-wave Doppler from the RVOT may provide surrogate findings for elevated PVR in the form of a triangular envelope with late-systolic notching or a more pronounced mid-systolic notching pattern.[29]

The European Society of Cardiology (ESC) and the European Respiratory Society (ERS) guidelines recommend using only the peak TR velocity to avoid inaccuracies associated with RA pressure estimations based on inferior vena cava (IVC) diameter. Furthermore, using peak TR velocity and other echocardiographic signs for PH, the echocardiographic probability of PH can be determined in symptomatic patients (Table 8A–B).[30] In addition to hemodynamic assessment, echocardiography enables identification of conditions that may predispose to pulmonary hypertension (Table 9). For example, the presence of significant left-sided valve disease or the presence of left ventricular systolic or diastolic dysfunction would favor a postcapillary mechanism for pulmonary hypertension (group 2, PH secondary to left heart disease). If such findings are absent and the probability of PH is high based on symptoms and echocardiographic assessment, diagnostic workup should focus on precapillary causes of pulmonary hypertension that include pulmonary arterial hypertension (group 1), PH secondary to lung disease (group 3), and chronic thromboembolic pulmonary hypertension (CTEPH) (group 4). A subgroup of patients with pulmonary venous hypertension from left heart disease (group 2) may eventually develop "reactive" pulmonary arterial vasoconstriction and remodeling.[31] In systemic sclerosis, pulmonary arterial hypertension may coexist with pulmonary venous hypertension secondary to LV diastolic dysfunction.

Echocardiography during exercise to assess for exercise-induced pulmonary hypertension may be considered in patients with exertional dyspnea that have an intermediate echocardiographic probability of pulmonary hypertension (Table 8A). However, the natural history of this entity remains to be established, and no specific therapeutic recommendations exist. A semi-recumbent exercise is preferred to facilitate optimal acquisition, although upright exercise may be considered if the resting TR Doppler signal was of high quality.[32] Of note, the upper limit of normal for exercise-induced increase in

TABLE 9 Causes of pulmonary hypertension identified by echocardiography[25]

Conditions that predispose to pulmonary hypertension
• Congenital or acquired valvular disease (MR, MS, AS, prosthetic valve dysfunction).
• Left ventricular systolic dysfunction.
• Impaired left ventricular diastolic function (hypertensive heart disease, HCM, Fabry's disease, infiltrative cardiomyopathies).
• Other obstructive lesions (coarctation, supravalvular AS, subaortic membrane, cor triatriatum)
• Congenital disease with shunt (ASD, VSD, coronary fistula, patent ductus arteriosus, anomalous pulmonary venous return).
• Pulmonary embolus (thrombus in IVC, right-sided cardiac chamber, or PA; tricuspid or pulmonic valve vegetation).
• Pulmonary vein thrombosis/stenosis.
Findings that suggest specific disease entity
• Left-sided valve changes (SLE, anorexigen use)
• Intra-pulmonary shunts (hereditary hemorrhagic telangiectasia)
• Pericardial effusion (IPAH, SLE, systemic sclerosis)

AS=aortic stenosis; ASD=atrial septal defect; HCM=hypertrophic cardiomyopathy; IPAH=idiopathic pulmonary arterial hypertension; IVC=inferior vena cava; MR=mitral regurgitation; MS=mitral stenosis; PA=pulmonary artery; SLE=systemic lupus erythematosus; and VSD=ventricular septal defect.
Reproduced with permission from Elsevier.[25]

PA systolic pressure is variable based on the population studied, <40–45 mm Hg for normal healthy nonathletic and <55–60 mm Hg for highly conditioned athletes.[24,33,34] Therefore, exercise-induced changes in PA systolic pressure need to be interpreted with caution considering age, body mass index, gender, and endurance level of the patient.[24] In patients with established severe precapillary PH, exercise testing may be helpful to indirectly assess for RV systolic function (contractile reserve) based on exercise-induced increase in PA systolic pressure, values >30 mm Hg indicating good RV function.[35]

Tissue Doppler imaging, 2D strain imaging, and real-time 3D echocardiography have been utilized to assess RV function in the PAH population in several studies.[24] Decreased RV free wall and GLS in the setting of PH, and mostly PAH have been associated with clinical deterioration and higher mortality.[36–38] Table 10 lists several other echocardiographic predictors of prognosis in patients with PAH. Real-time 3D echocardiography offers better assessment of morphological changes in PH of diverse etiologies. Using 3D echocardiography, Grapsa et al. found PAH patients to have more pronounced adverse remodeling when compared with chronic CTEPH and PH secondary to mitral regurgitation (MR).[39] Tricuspid valve mobility was notably most restricted with CTEPH, while tricuspid valve tenting height and volume was increased in PAH and CTEPH but not with MR.[39] Sukmawan et al. similarly reported on the usefulness of 3D echocardiography in the assessment of tricuspid valve geometry in PH.[40]

8.3 | Pulmonary embolism

Acute pulmonary embolism (PE) is a medical emergency with an approximately 10% morality rate at 3 months.[41] In the absence of hemodynamic instability, the presence of RV dysfunction is an important predictor of adverse clinical outcomes ("intermediate-risk" or "submassive" PE).[42] In this subgroup of patients with acute pulmonary embolism, the use of fibrinolytic therapy prevented hemodynamic deterioration in comparison with unfractionated heparin (Pulmonary Embolism Thrombolysis—PLEITHO trial).[41] The echocardiographic criteria used to diagnose RV dysfunction included at least one of the following: RV end-diastolic diameter >30 mm (PLAX or short axis), RV to LV end-diastolic diameter ratio >0.9 (apical or subcostal four-chamber view), RV free wall hypokinesis, and peak TR velocity >2.6 m/s.[41]

Echocardiographic findings considered typical for acute PE include McConnell sign, the "60/60" sign, and presence of right heart thrombus.[43] These findings are not sufficiently sensitive to be used as primary criteria for therapeutic decision making.[44] McConnell sign refers to the distinct regional mid-basal RV free wall hypokinesis with preserved apical RV segment contraction in the setting of acute PE (Figure 7 A).[45] Although previously thought to be unique for acute PE, RV global and RV free wall longitudinal strain imaging data demonstrate a global reduction in strain magnitude (apex, mid, and base), with no evidence for apical sparing.[46] The 60/60 sign is described by the combined findings of RV acceleration time <60 ms (by pulsed-wave Doppler at RVOT with sweep speed of 100 cms^{-1}) and peak TR pressure gradient <60 mm Hg (Figure 7B and C).[44,47] In a single-center study of 511 consecutive patients with confirmed PE using contrast enhanced multidetector computed tomography (MDCT), the echocardiographic parameters to assess RV are presented in Table 11.[43] Patients with hemodynamically unstable (high-risk) PE had significantly abnormal values.

As MDCT can readily assess for RV strain based on RV/LV dimension ratio (abnormal if >0.9),[48] the role of echocardiography in patients with hemodynamically stable PE was investigated by Barrios et al. in a cohort of 848 patients.[49] Using a combination of the simplified Pulmonary Embolism Severity Index (sPESI), MDCT, and echocardiography, it was found that MDCT evidence of RV enlargement had low specificity (44%). Furthermore, in patients with sPESI of 1 or greater, and RV enlargement by MDCT, the additional findings of RV overload by echocardiography was associated with a higher incidence of adverse events as measured by the composite of all-cause mortality or hemodynamic collapse or recurrent PE (16.3% vs 8.5%).[49] In another study, newer echocardiographic methods such as mid-RV free wall longitudinal strain and RV ejection fraction by 3D echocardiography were independent predictors of poor outcomes.[50]

8.4 | Adult congenital heart disease

The prevalence of congenital heart disease in the adult population is on the rise.[51] Progressive RV dysfunction in this setting predisposes to reduced functional capacity and increased risk of ventricular arrhythmia.[52] As RV adapts well to chronic volume and pressure overload, the diagnosis of RV dysfunction is often delayed. Common congenital conditions associated with RV volume overload include atrial

TABLE 10 Echocardiographic prognostic predictors in patients with pulmonary arterial hypertension[24]

Study (Year of publication)	Patients	Age (y)	Etiology	Treatment	Echocardiographic indices	Follow-up (median)	Outcome
Eysmann et al. (1989)[77]	26 (18 women)	40.8	PPH	Vasodilators[a]	Pericardial effusion	19.7 mo	Death
Hinderliter et al. (1997)[78]	79 (57 women)	-	PPH	PGI	Pericardial effusion	1 y	Death, lung transplantation
Yeo et al. (1998)[79]	53 (38 women)	45±14	PPH	CCBs	Tei index[b] ≥0.83	2.9 y	Death, lung transplantation
Raymond et al. (2002)[80]	81 (59 women)	40±15	PPH	PGI	Pericardial effusion, RA area index (5 cm^2/m)	1 y	Death, lung transplantation
Forfia et al. (2006)[81]	63 (52 women)	55±15	IPAH, SSc, CTD, RD, CTEPH	PGI, ERA, PDE5-i inhibitors	TAPSE < 1.8 cm	19.3 mo	Death
Mahapatra et al. (2006)[82]	54 (41 women)	44±11	PPH	PGI, ERA, CCBs	PVCAP	49.3 mo	Death
Brierre et al. (2010)[83]	79 (36 women)	61.4	IPAH, anorexigens, SSc, IDD, portal hypertension, HIV, RD, CTEPH, sarcoidosis	ERA, PGI, PDE5-i inhibitors, PEA	MPAP ≥49 mm Hg, DPAP ≥29 mm Hg, abnormal EDSC, IVC diameter[c], Tei index[b] ≥0.98, TAPSE[d], pericardial effusion	12 mo	Death
Ghio et al. (2011)[84]	72 (52 women)	52±16	IPAH	According to current guidelines	RV diameters[e] (>36.5 mm)	38 mo	Death
Sachdev et al. (2011)[37]	80 (61 women)	56±14	PAH	According to current guidelines	RV free wall strain per absolute 5% decrease	24 mo	Death

CCB=calcium channel blocker; CTD=connective tissue disease; CTEPH=chronic thromboembolic pulmonary hypertension; DPAP=diastolic PAP as measured from pulmonary regurgitant flow; ERA=endothelin receptor antagonist (bosentan); EDSC=end-diastolic septal curve, defined as abnormal if convex toward the right ventricle on the two-dimensional parasternal short-axis view; HIV=human immunodeficiency virus; IDD=immune dysfunction disease; IVC=inferior vena cava; PDE5-i=phosphodiesterase type 5 inhibitor (sildenafil); PEA=pulmonary endarterectomy; PGI=prostacyclin and analogues (epoprostenol, iloprost, treprostinil); PPH=primary pulmonary hypertension; PVCAP=pulmonary vascular capacitance; RA=right atrial; RD=respiratory disease; SSc=systemic sclerosis (scleroderma); TAPSE=tricuspid annular plane systolic excursion.

[a]CCBs, prazosin, hydralazine.

[b]Tei index=(isovolumic contraction time+isovolumic relaxation time)/ejection time.

[c]Twenty or more millimeters with respiratory variation in IVC diameter <50%.

[d]As a continuous variable for each 1-mm decrease.

[e]RV end-diastolic diameters (RV wall thickness ≤6.6 mm) in the parasternal long-axis view.

Reproduced with permission from Elsevier.[24]

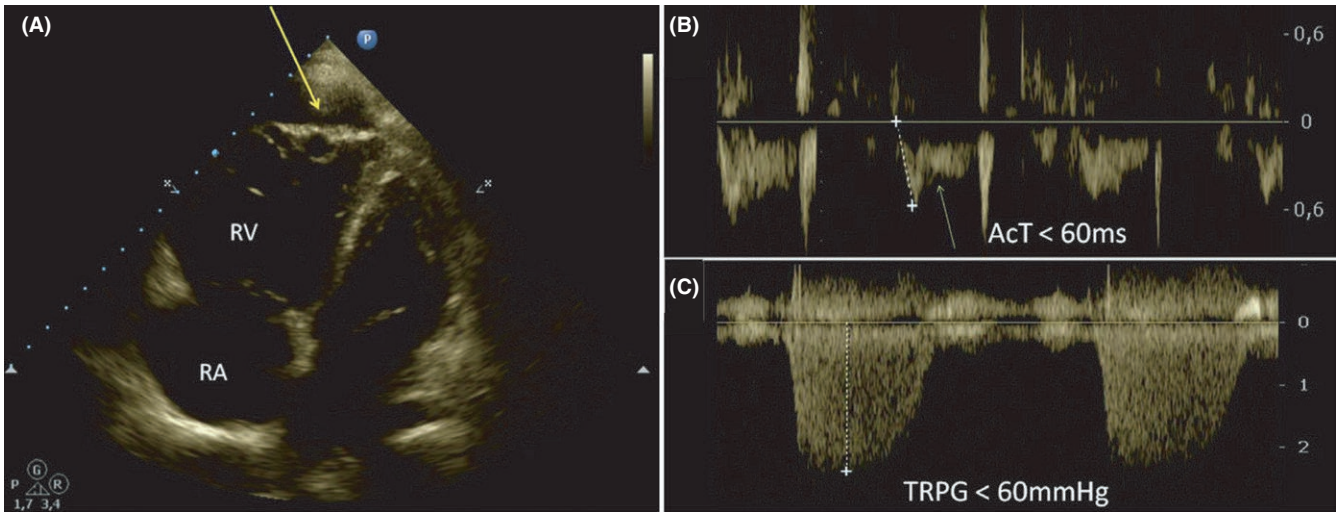

FIGURE 7 The McConnell sign (A). Hypokinesis of right ventricle free wall with a normal contraction of the apical segment (arrow). RA, right atrium; RV, right ventricle. The 60/60 sign. Coexistence of shortened PA acceleration time <60 ms (B) with mid-systolic notch (arrow) and of tricuspid regurgitation pressure gradient (TRPG) <60 mm Hg (C). Reproduced with permission from Elsevier[43]

TABLE 11 Echocardiographic parameters of 511 patients with confirmed PE according to the severity of PE[43]

Parameter	All PE (n=511)	High-risk PE (n=16)	Non-high-risk PE (n=495)	*P*
LV dimension (mm)	41.5±6.8	38.1±11.0	41.6±6.5	.19
RV dimension (mm)	38.3±8.1	45.0±8.3	38.0±8.0	**.004**
RV/LV	0.94±0.3	1.3±0.4	0.92±0.3	**.003**
TRPG (mm Hg)	34.4±16.4	49.2±22.3	33.9±16.0	**.02**
AcT (ms)	87.4±28.8	60.6±12.6	88.3±28.8	**<.0001**
TAPSE (mm)	21.2±5.8	16.5±4.9	21.3±5.8	**.40**
Flattened IVS	94 (18.4)	11 (68.8)	83 (16.8)	**<.0001**
RVD[a]	102 (20)	13 (81.2)	89 (18.0)	**<.0001**
McConnell sign	101 (19.8)	12 (75.0)	89 (18.0)	**.0003**
RiHT	9 (1.8)	3 (18.8)	6 (1.2)	**<.0001**
60/60 sign	66 (12.9)	5 (31.2)	61 (12.3)	.14
Distended IVC	66 (12.9)	3 (18.7)	63 (12.7)	.80

IVS=interventricular septum; RiHT=right heart thrombus; TAPSE=tricuspid annular plane systolic excursion; AcT=pulmonary ejection acceleration time. Data are expressed as mean±SD or as number (percentage). Statistically significant *P*-values are in boldface type.

[a]RVD was diagnosed when RV free wall hypokinesis was present and RV to LV end-diastolic ratio was >0.9 in the four-chamber apical view. Reproduced with permission from Elsevier.[43]

septal defect (ASD), pulmonary regurgitation typically in the setting of repaired tetralogy of Fallot (TOF) and TR with Ebstein's anomaly. Pressure overload commonly occurs with pulmonary valve stenosis, infundibular subpulmonary stenosis characteristic for TOF, and congenitally corrected transposition of the great arteries (TGA) because RV functions as the systemic ventricle.[53]

Unrepaired ASD is one of the most common congenital heart diseases encountered in the adult population. The diagnosis is often readily established by echocardiographic demonstration of interatrial shunting and evidence of RV volume overload. However, an isolated RV volume overload necessitates further investigation to identify the less common sinus venosus or unroofed coronary sinus subtypes of atrial septal communications.[54] The sinus venosus defect is frequently associated with partial anomalous pulmonary venous connection. Transesophageal echocardiography preferably with real-time 3D imaging is a valuable tool in the comprehensive assessment of ASD.[54] Regardless of symptoms, the presence of RV enlargement based on linear dimensions or RV volume estimation warrants ASD closure.[55] The most common cyanotic congenital heart disease is TOF. The tetrad consists of subpulmonary infundibular stenosis, ventricular septal defect, overriding aorta, and RV hypertrophy. Except for the rare TOF patient that has a mild degree of subpulmonary

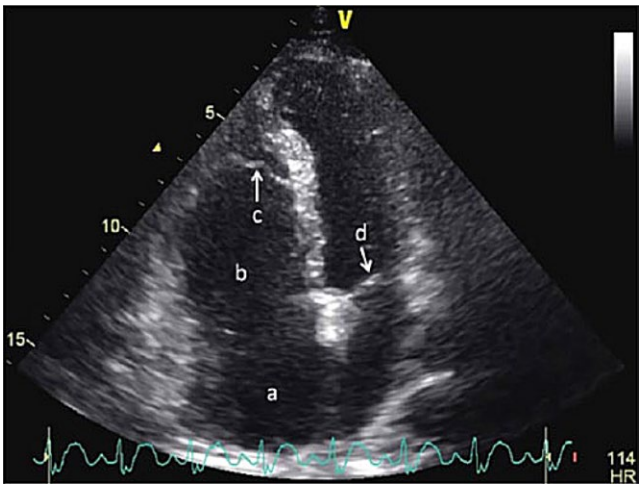

FIGURE 8 Echocardiography (apical four-chamber view) showing features of Ebstein's anomaly (a=right atrium; b=dilated atrialized portion of right ventricle; c=downward displacement of tricuspid valve; d=mitral valve. Reproduced under the terms of Creative Commons Attribution 3.0 License, (http://www.creativecommons.org/licenses/by/3.0/): Acharya P, et al. Ebstein Anomaly With QRS Fragmentation on Electrocardiogram. Journal of investigative medicine high impact case reports. Jan-Mar 2017;5(1):2324709616688710. (http://journals.sagepub.com/doi/full/10.1177/2324709616688710)

stenosis, almost all adults with TOF are seen postoperatively. In contrast to the unoperated TOF patient with RV pressure overload, operated patients are at risk of RV volume overload from residual pulmonary regurgitation. This postoperative sequela results from the use of RVOT patch to relieve the subpulmonary obstruction.[52] Additionally, pulmonary valvotomy or valvectomy if performed results in pulmonary regurgitation. In the long term, untreated pulmonary regurgitation leads to severe RV dysfunction. Pulmonary valve replacement is recommended in the operated TOF patient for severe pulmonary regurgitation if accompanied by symptoms or in the presence of moderate to severe RV enlargement or RV dysfunction.[55] Ebstein's anomaly is characterized by apical displacement of both the septal and the posterior tricuspid leaflets of >20 mm or 8 mm/m^2 in adults (Figure 8).[56] Moderate to severe TR and associated pathology such as ASD, if present, often result in RV volume overload in Ebstein's anomaly.

Transposition of the great arteries in the adult population comprises of two subgroups of patients: (1) repaired dextrotransposition of the great arteries (d-TGA) characterized by atrioventricular concordance and ventriculoarterial discordance (aorta originates from RV and pulmonary artery from LV), and (2) congenitally corrected transposition of the great arteries (l-TGA) with double discordance (morphological RV functions as the systemic ventricle). The arterial switch operation is the procedure of choice for d-TGA. Echocardiographic follow-up after arterial switch should focus on arterial anastomotic site stenoses, aortic root enlargement, and native pulmonary valve regurgitation (neoaortic valve).[55,57,58] Adult patients that underwent the older atrial baffle procedures (Mustard or Senning) are frequently encountered in clinical practice. With the atrial baffles, the major issues are obstruction and shunting resulting from baffle leaks. In the long term, baffle procedures result in RV failure from chronic exposure to systemic pressures. The use of agitated saline contrast enables comprehensive assessment of the intraatrial baffle anatomy and hemodynamics.[55] TEE is also frequently used in this situation to improve assessment.

TABLE 12 Revised Task Force Criteria for the diagnosis of Arrhythmogenic Right Ventricular Cardiomyopathy/Dysplasia by 2D Echocardiography[63]

Major criteria[a]
Regional RV akinesia, dyskinesia, or aneurysm *and* 1 of the following (end-diastole):[b]
• PLAX RVOT ≥32 mm (corrected for body size PLAX/BSA ≥19 mm/m^2) • PSAX RVOT ≥36 mm (corrected for body size PSAX/BSA ≥21 mm/m^2) • *or* fractional area change ≤33%
Minor criteria[a]
Regional RV akinesia or dyskinesia *and* 1 of the following (end-diastole):[b]
• PLAX RVOT ≥29 to <32 mm (corrected for body size PLAX/BSA ≥16 to <19 mm/m^2) • PSAX RVOT ≥32 to <36 mm (corrected for body size PSAX/BSA ≥18 to <21 mm/m^2) • *or* fractional area change >33%≤-40%

PLAX=parasternal long-axis view; RVOT=RV outflow tract; BSA=body surface area; PSAX=parasternal short-axis view.
[a]Diagnostic terminology for revised criteria: definite diagnosis: two major or one major and two minor criteria or four minor from different categories; borderline: one major and one minor or three minor criteria from different categories; possible: one major or two minor criteria from different categories.
[b]Hypokinesis is not included in the definitions of RV regional wall-motion abnormalities.

8.5 | Arrhythmogenic right ventricular cardiomyopathy (ARVC)

The histopathological hallmark of ARVC is progressive replacement of the RV myocardium by fibrous and fatty tissue that is caused by a genetic defect involving the cardiac desmosomes.[59] The "triangle of dysplasia" formed by the RV inflow (particularly the inferior wall below the tricuspid valve), apex, and infundibulum is often the site for right ventricular aneurysm formation.[60] Right ventricular aneurysm in this location is considered pathognomonic for ARVC.[61] However, more commonly, echocardiography would reveal significantly increased RVOT dimensions and reduced FAC.[62] The RVOT dimension is particularly important as enlargement is commonly noted at this level.[62] Other morphologic findings include deranged RV trabecula and sacculations. The major and minor Revised Task Force Criteria for the diagnosis of ARVC by 2D echocardiography are presented in Table 12.[63] Figure 9 depicts several 2D echocardiographic findings that may be seen in ARVC.

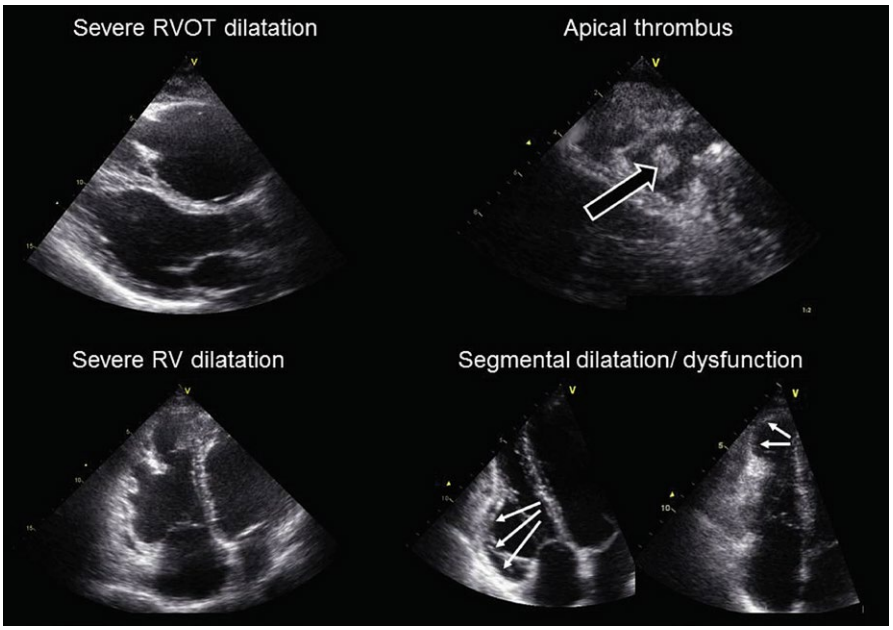

FIGURE 9 Conventional echocardiography in arrhythmogenic right ventricular dysplasia or cardiomyopathy (ARVD/C). Left upper: PLAX, severe RVOT dilatation (57 mm, 27.4 mm/m^2) in 57-year-old ARVD/C patient; Right upper: RV SAX, apical thrombus in 16-year-old ARVD/C patient, RV-FAC was 29%; left lower: apical four-chamber view, severe dilatation of RV, RVIT=49 mm, and hyperreflective moderator band; right lower: apical four-chamber view, apical aneurysm, and segmental subtricuspid dilatation. PLAX=parasternal long-axis view; RVOT=right ventricular outflow tract; RV=right ventricle; SAX=short-axis view; RV-FAC=right ventricular-fractional area change; RVIT=right ventricular inflow tract. Reproduced under the terms of open access Creative Common Attribution-Non Commercial-No Derivatives 4.0 International (CC BY-NC-ND 4.0): Mast TP, Teske AJ, Doevendans PA, Cramer MJ. Current and future role of echocardiography in arrhythmogenic right ventricular dysplasia/cardiomyopathy. Cardiology Journal. 2015;22(4):362–374. (http://journals.viamedica.pl/cardiology_journal/article/view/CJ.a2015.0018/30407)

TABLE 13 Echocardiographic markers to identify RV MI in the setting of acute inferior MI[2]

Echocardiographic measurement	Involvement of right ventricle
TAPSE<10 mm	75% positive predictive value for diagnosis of RV MI[85]
S′< 12 cm/s	81% sensitivity and 82% specificity for diagnosis of RV MI
	63% sensitivity and 88% specificity for diagnosis of proximal RCA disease[86]
S′< 8 cm/s	78% sensitivity and 86% specificity for diagnosis of RV MI[68]
MPI>0.7	94% sensitivity and 80% specificity for diagnosis of RV MI
	78% sensitivity and 91% specificity for diagnosis of proximal RCA disease[86]
S′/MPI<17	85% sensitivity and 87% specificity for diagnosis of proximal RCA disease[87]
RV ejection fraction<51%	91% sensitivity and 80% specificity for diagnosis of RV MI[88]

RV=right ventricle; MPI=RV myocardial performance index; TAPSE=tricuspid annular plane systolic excursion. Published with permission from Elsevier.[2]

8.6 | RV myocardial infarction

In the setting of inferior wall myocardial infarction, concomitant RV myocardial infarction (RVMI) incurs an increased risk for all-cause mortality, shock, and ventricular arrhythmia.[64] RVMI without LV involvement is rare with atherosclerotic coronary artery disease.[65] Significant RV hypertrophy may predispose to RV ischemia or infarction in the absence of significant coronary disease.[66] Data on echocardiographic measurements to identify RVMI in acute inferior wall MI are summarized in Table 13. RV enlargement, paradoxical septal

motion, and TR are additional findings. Of prognostic value, TAPSE ≤15 mm, lateral tricuspid annulus S'<8 cm/s, RV-FAC (<32%), and peak systolic longitudinal strain of the RV free wall (≥−22.1%) have been associated with all-cause mortality.[67–69] Regional RV wall-motion abnormalities are frequently noted with RVMI, and the segments involved are described as shown in Figure 2.[70] An elevated right atrial pressure with RVMI is indicative for significant RV dysfunction and therefore is more frequently associated with RV regional wall-motion abnormalities involving multiple segments.[71]

9 | CONCLUSIONS

With the available clinical and imaging data in both normal and diseased population, a transition from qualitative to quantitative assessment of the RV is possible in today's clinical practice. A standardized approach that includes obtaining the RV-focused apical four-chamber view is an essential first step to reliably estimate linear dimensions. This should be followed by an assessment of RV function using nonvolumetric surrogate measurements. These techniques are feasible in most laboratories. Whenever possible, acquiring more than one parameter of RV function by 2D echocardiography improves interpretation. The increasing availability of 3D echocardiography is an important step forward in our ability to directly measure RV volume and function. Clinical situations where therapeutic decision making relies upon RV size and function may now be adequately addressed using available echocardiographic techniques, in the absence of limitations posed by image quality.

REFERENCES

1. Rudski LG, Lai WW, Afilalo J, et al. Guidelines for the echocardiographic assessment of the right heart in adults: a report from the American Society of Echocardiography endorsed by the European Association of Echocardiography, a registered branch of the European Society of Cardiology, and the Canadian Society of Echocardiography. *J Am Soc Echocardiogr*. 2010;23:685–713; quiz 786-688.
2. Rallidis LS, Makavos G, Nihoyannopoulos P. Right ventricular involvement in coronary artery disease: role of echocardiography for diagnosis and prognosis. *J Am Soc Echocardiogr*. 2014;27:223–229.
3. Lang RM, Badano LP, Mor-Avi V, et al. Recommendations for cardiac chamber quantification by echocardiography in adults: an update from the American Society of Echocardiography and the European Association of Cardiovascular Imaging. *J Am Soc Echocardiogr*. 2015;28:1–39 e14.
4. Grifoni S, Olivotto I, Cecchini P, et al. Short-term clinical outcome of patients with acute pulmonary embolism, normal blood pressure, and echocardiographic right ventricular dysfunction. *Circulation*. 2000;101:2817–2822.
5. Vivo RP, Cordero-Reyes AM, Qamar U, et al. Increased right-to-left ventricle diameter ratio is a strong predictor of right ventricular failure after left ventricular assist device. *J Heart Lung Transplant*. 2013;32:792–799.
6. Shimada YJ, Shiota M, Siegel RJ, Shiota T. Accuracy of right ventricular volumes and function determined by three-dimensional echocardiography in comparison with magnetic resonance imaging: a meta-analysis study. *J Am Soc Echocardiogr*. 2010;23:943–953.
7. Sugeng L, Mor-Avi V, Weinert L, et al. Multimodality comparison of quantitative volumetric analysis of the right ventricle. *JACC Cardiovasc Imaging*. 2010;3:10–18.
8. Reynertson SI, Kundur R, Mullen GM, Costanzo MR, McKiernan TL, Louie EK. Asymmetry of right ventricular enlargement in response to tricuspid regurgitation. *Circulation*. 1999;100:465–467.
9. Jurcut R, Giusca S, La Gerche A, Vasile S, Ginghina C, Voigt JU. The echocardiographic assessment of the right ventricle: what to do in 2010? *Eur J Echocardiogr*. 2010;11:81–96.
10. Ryan T, Petrovic O, Dillon JC, Feigenbaum H, Conley MJ, Armstrong WF. An echocardiographic index for separation of right ventricular volume and pressure overload. *J Am Coll Cardiol*. 1985;5:918–927.
11. Holman WL, Kormos RL, Naftel DC, et al. Predictors of death and transplant in patients with a mechanical circulatory support device: a multi-institutional study. *J Heart Lung Transplant*. 2009;28:44–50.
12. Kirklin JK, Naftel DC, Kormos RL, et al. Fifth INTERMACS annual report: risk factor analysis from more than 6,000 mechanical circulatory support patients. *J Heart Lung Transplant*. 2013;32:141–156.
13. Khazanie P, Rogers JG. Patient selection for left ventricular assist devices. *Congest Heart Fail*. 2011;17:227–234.
14. Stainback RF, Estep JD, Agler DA, et al. Echocardiography in the Management of Patients with Left Ventricular Assist Devices: recommendations from the American Society of Echocardiography. *J Am Soc Echocardiogr*. 2015;28:853–909.
15. Kiernan MS, French AL, DeNofrio D, et al. Preoperative three-dimensional echocardiography to assess risk of right ventricular failure after left ventricular assist device surgery. *J Cardiac Fail*. 2015;21:189–197.
16. Fitzpatrick JR 3rd, Frederick JR, Hiesinger W, et al. Early planned institution of biventricular mechanical circulatory support results in improved outcomes compared with delayed conversion of a left ventricular assist device to a biventricular assist device. *J Thorac Cardiovasc Surg*. 2009;137:971–977.
17. Argiriou M, Kolokotron SM, Sakellaridis T, et al. Right heart failure post left ventricular assist device implantation. *J Thorac Dis*. 2014;6(Suppl 1):S52–S59.
18. Grant AD, Smedira NG, Starling RC, Marwick TH. Independent and incremental role of quantitative right ventricular evaluation for the prediction of right ventricular failure after left ventricular assist device implantation. *J Am Coll Cardiol*. 2012;60:521–528.
19. Goldraich L, Kawajiri H, Foroutan F, et al. Tricuspid Valve Annular Dilation as a Predictor of Right Ventricular Failure After Implantation of a Left Ventricular Assist Device. *J Card Surg*. 2016;31:110–116.
20. Kato TS, Jiang J, Schulze PC, et al. Serial echocardiography using tissue Doppler and speckle tracking imaging to monitor right ventricular failure before and after left ventricular assist device surgery. *JACC. Heart Fail*. 2013;1:216–222.
21. Lampert BC, Teuteberg JJ. Right ventricular failure after left ventricular assist devices. *J Heart Lung Transplant*. 2015;34:1123–1130.
22. Patangi SO, George A, Pauli H, et al. Management issues during HeartWare left ventricular assist device implantation and the role of transesophageal echocardiography. *Ann Card Anaesth*. 2013;16:259–267.
23. Fida N, Loebe M, Estep JD, Guha A. Predictors and management of right heart failure after left ventricular assist device implantation. *Methodist Debakey Cardiovasc J*. 2015;11:18–23.
24. Bossone E, D'Andrea A, D'Alto M, et al. Echocardiography in pulmonary arterial hypertension: from diagnosis to prognosis. *J Am Soc Echocardiogr*. 2013;26:1–14.
25. McLaughlin VV, Archer SL, Badesch DB, et al. ACCF/AHA 2009 expert consensus document on pulmonary hypertension a report of the American College of Cardiology Foundation Task Force on Expert Consensus Documents and the American Heart Association developed in collaboration with the American College of Chest Physicians; American Thoracic Society, Inc.; and the Pulmonary Hypertension Association. *J Am Coll Cardiol*. 2009;53:1573–1619.

26. McQuillan BM, Picard MH, Leavitt M, Weyman AE. Clinical correlates and reference intervals for pulmonary artery systolic pressure among echocardiographically normal subjects. *Circulation*. 2001;104:2797–2802.
27. Abbas AE, Fortuin FD, Schiller NB, Appleton CP, Moreno CA, Lester SJ. A simple method for noninvasive estimation of pulmonary vascular resistance. *J Am Coll Cardiol*. 2003;41:1021–1027.
28. Haddad F, Zamanian R, Beraud AS, et al. A novel non-invasive method of estimating pulmonary vascular resistance in patients with pulmonary arterial hypertension. *J Am Soc Echocardiogr*. 2009;22:523–529.
29. Roberts JD, Forfia PR. Diagnosis and assessment of pulmonary vascular disease by Doppler echocardiography. *Pulm Circ*. 2011;1:160–181.
30. Galie N, Humbert M, Vachiery JL, et al. 2015 ESC/ERS Guidelines for the diagnosis and treatment of pulmonary hypertension: The Joint Task Force for the Diagnosis and Treatment of Pulmonary Hypertension of the European Society of Cardiology (ESC) and the European Respiratory Society (ERS): endorsed by: association for European Paediatric and Congenital Cardiology (AEPC), International Society for Heart and Lung Transplantation (ISHLT). *Eur Heart J*. 2016;37:67–119.
31. Rose-Jones LJ, McLaughlin VV. Pulmonary hypertension: types and treatments. *Curr Cardiol Rev*. 2015;11:73–79.
32. van Riel AC, Opotowsky AR, Santos M, et al. Accuracy of Echocardiography to Estimate Pulmonary Artery Pressures With Exercise: A Simultaneous Invasive-Noninvasive Comparison. *Circ Cardiovasc Imaging*. 2017;10(4):e005711.
33. Argiento P, Chesler N, Mule M, et al. Exercise stress echocardiography for the study of the pulmonary circulation. *Eur Respir J*. 2010;35:1273–1278.
34. Bossone E, Rubenfire M, Bach DS, Ricciardi M, Armstrong WF. Range of tricuspid regurgitation velocity at rest and during exercise in normal adult men: implications for the diagnosis of pulmonary hypertension. *J Am Coll Cardiol*. 1999;33:1662–1666.
35. Grunig E, Tiede H, Enyimayew EO, et al. Assessment and prognostic relevance of right ventricular contractile reserve in patients with severe pulmonary hypertension. *Circulation*. 2013;128:2005–2015.
36. Haeck ML, Scherptong RW, Marsan NA, et al. Prognostic value of right ventricular longitudinal peak systolic strain in patients with pulmonary hypertension. *Circ Cardiovasc Imaging*. 2012;5:628–636.
37. Sachdev A, Villarraga HR, Frantz RP, et al. Right ventricular strain for prediction of survival in patients with pulmonary arterial hypertension. *Chest*. 2011;139:1299–1309.
38. Park JH, Park MM, Farha S, et al. Impaired Global Right Ventricular Longitudinal Strain Predicts Long-Term Adverse Outcomes in Patients with Pulmonary Arterial Hypertension. *J Cardiovasc Ultrasound*. 2015;23:91–99.
39. Grapsa J, Gibbs JS, Dawson D, et al. Morphologic and functional remodeling of the right ventricle in pulmonary hypertension by real time three dimensional echocardiography. *Am J Cardiol*. 2012;109:906–913.
40. Sukmawan R, Watanabe N, Ogasawara Y, et al. Geometric changes of tricuspid valve tenting in tricuspid regurgitation secondary to pulmonary hypertension quantified by novel system with transthoracic real-time 3-dimensional echocardiography. *J Am Soc Echocardiogr*. 2007;20:470–476.
41. Meyer G, Vicaut E, Danays T, et al. Fibrinolysis for patients with intermediate-risk pulmonary embolism. *N Engl J Med*. 2014;370:1402–1411.
42. Jaff MR, McMurtry MS, Archer SL, et al. Management of massive and submassive pulmonary embolism, iliofemoral deep vein thrombosis, and chronic thromboembolic pulmonary hypertension: a scientific statement from the American Heart Association. *Circulation*. 2011;123:1788–1830.
43. Kurnicka K, Lichodziejewska B, Goliszek S, et al. Echocardiographic Pattern of Acute Pulmonary Embolism: analysis of 511 Consecutive Patients. *J Am Soc Echocardiogr*. 2016;29:907–913.
44. Kurzyna M, Torbicki A, Pruszczyk P, et al. Disturbed right ventricular ejection pattern as a new Doppler echocardiographic sign of acute pulmonary embolism. *Am J Cardiol*. 2002;90:507–511.
45. McConnell MV, Solomon SD, Rayan ME, Come PC, Goldhaber SZ, Lee RT. Regional right ventricular dysfunction detected by echocardiography in acute pulmonary embolism. *Am J Cardiol*. 1996;78:469–473.
46. Mediratta A, Addetia K, Medvedofsky D, Gomberg-Maitland M, Mor-Avi V, Lang RM. Echocardiographic Diagnosis of Acute Pulmonary Embolism in Patients with McConnell's Sign. *Echocardiography*. 2016;33:696–702.
47. Torbicki A, Kurzyna M, Ciurzynski M, et al. Proximal pulmonary emboli modify right ventricular ejection pattern. *Eur Respir J*. 1999;13:616–621.
48. Schoepf UJ, Kucher N, Kipfmueller F, Quiroz R, Costello P, Goldhaber SZ. Right ventricular enlargement on chest computed tomography: a predictor of early death in acute pulmonary embolism. *Circulation*. 2004;110:3276–3280.
49. Barrios D, Morillo R, Lobo JL, et al. Assessment of right ventricular function in acute pulmonary embolism. *Am Heart J*. 2017;185:123–129.
50. Vitarelli A, Barilla F, Capotosto L, et al. Right ventricular function in acute pulmonary embolism: a combined assessment by three-dimensional and speckle-tracking echocardiography. *J Am Soc Echocardiogr*. 2014;27:329–338.
51. Marelli AJ, Ionescu-Ittu R, Mackie AS, Guo L, Dendukuri N, Kaouache M. Lifetime prevalence of congenital heart disease in the general population from 2000 to 2010. *Circulation*. 2014;130:749–756.
52. Warnes CA. Adult congenital heart disease importance of the right ventricle. *J Am Coll Cardiol*. 2009;54:1903–1910.
53. Davlouros PA, Niwa K, Webb G, Gatzoulis MA. The right ventricle in congenital heart disease. *Heart*. 2006;92(Suppl 1):i27–i38.
54. Silvestry FE, Cohen MS, Armsby LB, et al. Guidelines for the Echocardiographic Assessment of Atrial Septal Defect and Patent Foramen Ovale: From the American Society of Echocardiography and Society for Cardiac Angiography and Interventions. *J Am Soc Echocardiogr*. 2015;28:910–958.
55. Warnes CA, Williams RG, Bashore TM, et al. ACC/AHA 2008 Guidelines for the Management of Adults with Congenital Heart Disease: Executive Summary: a report of the American College of Cardiology/American Heart Association Task Force on Practice Guidelines (writing committee to develop guidelines for the management of adults with congenital heart disease). *Circulation*. 2008;118:2395–2451.
56. Oechslin E, Buchholz S, Jenni R. Ebstein's anomaly in adults: doppler-echocardiographic evaluation. *Thorac Cardiovasc Surg*. 2000;48:209–213.
57. Losay J, Touchot A, Serraf A, et al. Late outcome after arterial switch operation for transposition of the great arteries. *Circulation*. 2001;104(12 Suppl 1):I121–I126.
58. Formigari R, Toscano A, Giardini A, et al. Prevalence and predictors of neoaortic regurgitation after arterial switch operation for transposition of the great arteries. *J Thorac Cardiovasc Surg*. 2003;126:1753–1759.
59. Corrado D, Link MS, Calkins H. Arrhythmogenic Right Ventricular Cardiomyopathy. *N Engl J Med*. 2017;376:61–72.
60. Marcus FI, Fontaine GH, Guiraudon G, et al. Right ventricular dysplasia: a report of 24 adult cases. *Circulation*. 1982;65:384–398.
61. Basso C, Thiene G, Corrado D, Angelini A, Nava A, Valente M. Arrhythmogenic right ventricular cardiomyopathy. Dysplasia, dystrophy, or myocarditis? *Circulation*. 1996;94:983–991.
62. Yoerger DM, Marcus F, Sherrill D, et al. Echocardiographic findings in patients meeting task force criteria for arrhythmogenic right ventricular dysplasia: new insights from the multidisciplinary study of right ventricular dysplasia. *J Am Coll Cardiol*. 2005;45:860–865.
63. Marcus FI, McKenna WJ, Sherrill D, et al. Diagnosis of arrhythmogenic right ventricular cardiomyopathy/dysplasia: proposed modification of the task force criteria. *Circulation*. 2010;121:1533–1541.

64. Mehta SR, Eikelboom JW, Natarajan MK, et al. Impact of right ventricular involvement on mortality and morbidity in patients with inferior myocardial infarction. *J Am Coll Cardiol*. 2001;37:37–43.
65. Kinch JW, Ryan TJ. Right ventricular infarction. *N Engl J Med*. 1994;330:1211–1217.
66. Carlson EB, Reimer KA, Rankin JS, Peter RH, McCormack KM, Alexander LG. Right ventricular subendocardial infarction in a patient with pulmonary hypertension, right ventricular hypertrophy, and normal coronary arteries. *Clin Cardiol*. 1985;8:499–502.
67. Samad BA, Alam M, Jensen-Urstad K. Prognostic impact of right ventricular involvement as assessed by tricuspid annular motion in patients with acute myocardial infarction. *Am J Cardiol*. 2002;90:778–781.
68. Dokainish H, Abbey H, Gin K, Ramanathan K, Lee PK, Jue J. Usefulness of tissue Doppler imaging in the diagnosis and prognosis of acute right ventricular infarction with inferior wall acute left ventricular infarction. *Am J Cardiol*. 2005;95:1039–1042.
69. Antoni ML, Scherptong RW, Atary JZ, et al. Prognostic value of right ventricular function in patients after acute myocardial infarction treated with primary percutaneous coronary intervention. *Circ Cardiovasc Imaging*. 2010;3:264–271.
70. D'Arcy B, Nanda NC. Two-dimensional echocardiographic features of right ventricular infarction. *Circulation*. 1982;65:167–173.
71. Lopez-Sendon J, Garcia-Fernandez MA, Coma-Canella I, Yanguela MM, Banuelos F. Segmental right ventricular function after acute myocardial infarction: two-dimensional echocardiographic study in 63 patients. *Am J Cardiol*. 1983;51:390–396.
72. Puwanant S, Hamilton KK, Klodell CT, et al. Tricuspid annular motion as a predictor of severe right ventricular failure after left ventricular assist device implantation. *J Heart Lung Transplant*. 2008;27:1102–1107.
73. Potapov EV, Stepanenko A, Dandel M, et al. Tricuspid incompetence and geometry of the right ventricle as predictors of right ventricular function after implantation of a left ventricular assist device. *J Heart Lung Transplant*. 2008;27:1275–1281.
74. Kukucka M, Stepanenko A, Potapov E, et al. Right-to-left ventricular end-diastolic diameter ratio and prediction of right ventricular failure with continuous-flow left ventricular assist devices. *J Heart Lung Transplant*. 2011;30:64–69.
75. Kato TS, Farr M, Schulze PC, et al. Usefulness of two-dimensional echocardiographic parameters of the left side of the heart to predict right ventricular failure after left ventricular assist device implantation. *Am J Cardiol*. 2012;109:246–251.
76. Cameli M, Lisi M, Righini FM, et al. Speckle tracking echocardiography as a new technique to evaluate right ventricular function in patients with left ventricular assist device therapy. *J Heart Lung Transplant*. 2013;32:424–430.
77. Eysmann SB, Palevsky HI, Reichek N, Hackney K, Douglas PS. Two-dimensional and Doppler-echocardiographic and cardiac catheterization correlates of survival in primary pulmonary hypertension. *Circulation*. 1989;80:353–360.
78. Hinderliter AL, Willis PW, Barst RJ, et al. Effects of long-term infusion of prostacyclin (epoprostenol) on echocardiographic measures of right ventricular structure and function in primary pulmonary hypertension. Primary Pulmonary Hypertension Study Group. *Circulation* 1997;95:1479–1486.
79. Yeo TC, Dujardin KS, Tei C, Mahoney DW, McGoon MD, Seward JB. Value of a Doppler-derived index combining systolic and diastolic time intervals in predicting outcome in primary pulmonary hypertension. *Am J Cardiol*. 1998;81:1157–1161.
80. Raymond RJ, Hinderliter AL, Willis PW, et al. Echocardiographic predictors of adverse outcomes in primary pulmonary hypertension. *J Am Coll Cardiol*. 2002;39:1214–1219.
81. Forfia PR, Fisher MR, Mathai SC, et al. Tricuspid annular displacement predicts survival in pulmonary hypertension. *Am J Respir Crit Care Med*. 2006;174:1034–1041.
82. Mahapatra S, Nishimura RA, Oh JK, McGoon MD. The prognostic value of pulmonary vascular capacitance determined by Doppler echocardiography in patients with pulmonary arterial hypertension. *J Am Soc Echocardiogr*. 2006;19:1045–1050.
83. Brierre G, Blot-Souletie N, Degano B, Tetu L, Bongard V, Carrie D. New echocardiographic prognostic factors for mortality in pulmonary arterial hypertension. *Eur J Echocardiogr*. 2010;11:516–522.
84. Ghio S, Pazzano AS, Klersy C, et al. Clinical and prognostic relevance of echocardiographic evaluation of right ventricular geometry in patients with idiopathic pulmonary arterial hypertension. *Am J Cardiol*. 2011;107:628–632.
85. Shah AR, Grodman R, Salazar MF, Rehman NU, Coppola J, Braff R. Assessment of acute right ventricular dysfunction induced by right coronary artery occlusion using echocardiographic atrioventricular plane displacement. *Echocardiography*. 2000;17(6 Pt 1):513–519.
86. Ozdemir K, Altunkeser BB, Icli A, Ozdil H, Gok H. New parameters in identification of right ventricular myocardial infarction and proximal right coronary artery lesion. *Chest*. 2003;124:219–226.
87. Kakouros N, Kakouros S, Lekakis J, Rizos I, Cokkinos D. Tissue Doppler imaging of the tricuspid annulus and myocardial performance index in the evaluation of right ventricular involvement in the acute and late phase of a first inferior myocardial infarction. *Echocardiography*. 2011;28:311–319.
88. Kidawa M, Chizynski K, Zielinska M, Kasprzak JD, Krzeminska-Pakula M. Real-time 3D echocardiography and tissue Doppler echocardiography in the assessment of right ventricle systolic function in patients with right ventricular myocardial infarction. *Eur Heart J Cardiovasc Imaging*. 2013;14:1002–1009.

SUPPORTING INFORMATION

Additional Supporting Information may be found online in the supporting information tab for this article.

MOVIE S1 Three-dimensional (3D) right ventricular (RV) volumetric reconstruction in a healthy adult, generated using the 4D RV function software (TomTec Imaging Systems, Munich, Germany)

MOVIE S2 In contrast this movie demonstrates RV systolic dysfunction with reduced RV EF and abnormal strain values

MOVIE S3 Two-dimensional (2D) transesophageal echocardiography (TEE) obtained in a patient with advanced heart failure, following surgical implantation of the HeartWare left ventricular assist device (LVAD) system

MOVIE S4 (TEE, mid-esophageal four-chamber view) was obtained on postoperative day 2 after optimization of LVAD pump speed and initiation of inotropic medication

How to cite this article: Venkatachalam S, Wu G, Ahmad M. Echocardiographic assessment of the right ventricle in the current era: Application in clinical practice. *Echocardiography*. 2017;00:1–18. https://doi.org/10.1111/echo.13651